J. Fluid Mech. (1978), *vol.* 89, *part* 1, *pp.* 79–95
Printed in Great Britain

Shock waves at a slow-fast gas interface

By A. M. ABD-EL-FATTAH AND L. F. HENDERSON
Department of Mechanical Engineering, University of Sydney,
New South Wales 2006, Australia

(Received 7 February 1978)

This paper describes the results of our experiments with shock waves refracting at a CO_2/CH_4 interface. The refraction is slow–fast because the speed of sound in the incident gas (CO_2) is less than that in the transmitting gas (CH_4). We found three phenomena which apparently have not been reported before and which all have free precursor shocks in their wave systems; schlieren photographs of them are presented. As a result of the present and earlier work, we can assert that there exist at least four different free precursor refractions. Theoretical studies suggest that the slow–fast phenomena can be conveniently classified into three groups characterized by different ranges of values of the inverse strength ξ_i of the incident shock i. The classification may be an exhaustive list of the phenomena, at least when the gases are nearly perfect, but we cannot be sure. We present experimental data on all the phenomena in each group, including data on the transition conditions from one wave system to another both within and across the groups.

1. Introduction

In our 1976 paper (Abd-el-Fattah, Henderson & Lozzi 1976) we published data from our shock-tube experiments with shock waves refracting at the slow–fast CO_2/He interface. The experimental method was fully described in that paper; but briefly, the gases were initially prevented from mixing by a delicate polymer membrane which was about ten molecules thick. A plane shock i was then started in the CO_2 and refracted as it tore through the membrane and entered the He. There was significant leakage through the unruptured membrane, which caused mutual contamination of the gases before and during the passage of the shock. This effect was monitored by gas analysis equipment and the measured contamination was allowed for in our calculations. The reflected wave could be either a shock r or an expansion e, but we measured its wave angle ω_1' or ω_e, respectively, for a prescribed angle of incidence ω_0 (figure 1). The inverse strength of i was defined by $\xi_i \equiv P_0/P_1$, where P denotes the pressure and the subscripts 0 and 1 refer to the undisturbed and disturbed states of the CO_2 on either side of i. In all our 1976 experiments ξ_i was held constant at $\xi_i = 0{\cdot}5$. When i struck the interface at less than the critical angle $\omega_0 = 23{\cdot}1°$ we obtained the well-known regular refraction *RRE* where the reflected wave was an expansion. Its theory has been developed by Polachek & Seeger (1951), Jahn (1956) and Henderson (1967) and agreed well with the data. Between $\omega_0 = 23{\cdot}1°$ and a second critical angle $\omega_0 = 28{\cdot}8°$ we found an irregular system which we called a bound precursor refraction *BPR*. Although its transmitted shock t was always ahead of i it proceeded along the interface at very nearly the same velocity. For $\omega_0 > 28{\cdot}8°$, the velocity of t was greater

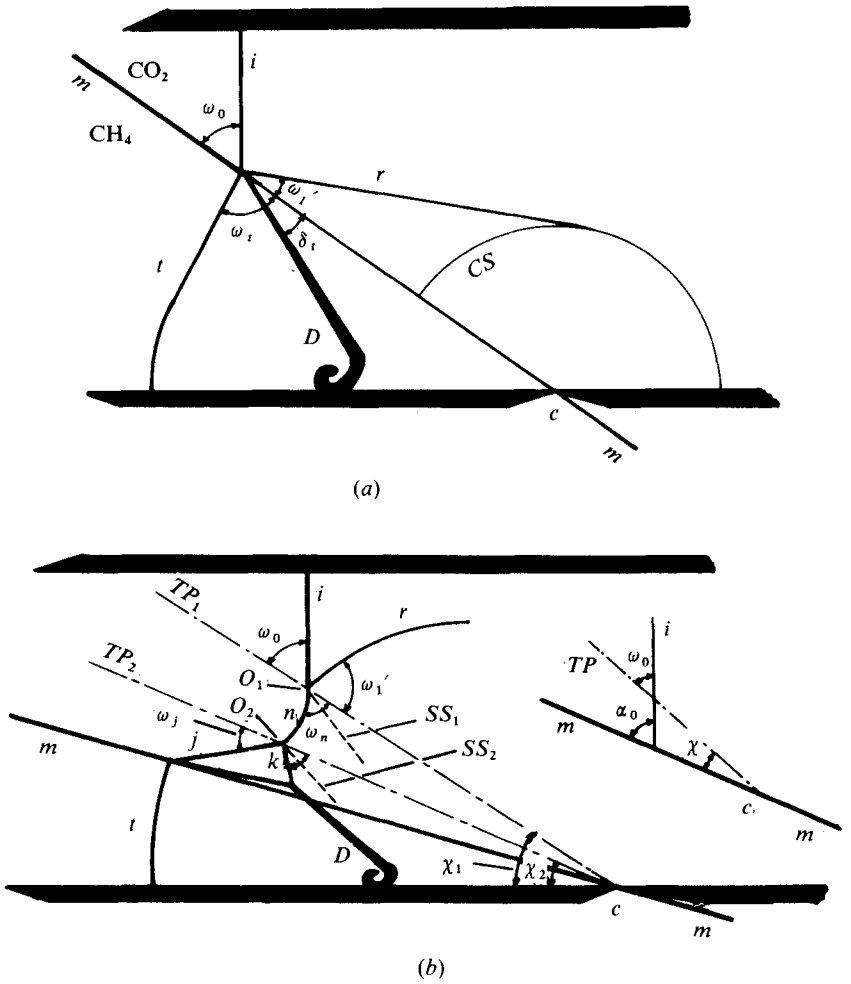

FIGURE 1. Nomenclature for the refraction of a plane shock wave at a CO_2/CH_4 interface. (*a*) Typical regular refraction ($\omega_0 = \alpha_0$). (*b*) Typical irregular refraction ($\omega_0 \neq \alpha_0$). *i*, incident shock; *r*, reflected shock; *t*, transmitted shock; *D*, deflected gas interface; *mm*, undisturbed gas interface; *C*, corner where refraction starts; *CS*, corner signal; *n*, Mach stem; *j*, free precursor shock (CO_2); *k*, modified Mach (or von Neumann) stem; $\chi_{1,2}$, trajectory path angles of shock wave confluences; $TP_{1,2}$, trajectory paths of the shock wave confluences; $SS_{1,2}$, slip-stream discontinuities; α_0, set angle of incidence with respect to the gas interface; ω_0, angle of incidence observed with respect to TP_1; ω_1', angle of shock reflexion measured from the same path as ω_0; ω_t, wave angle of *t*; δ_t, deflexion angle of the disturbed gas interface.

than that of *i* along the interface, and we called the resulting wave system a free precursor refraction *FPR*. We formulated a piston theory of the *FPR* system which agreed quite well with the data provided that the inertia of the membrane was taken into account, but there was no adequate theory for the *BPR* system.

In a later paper (Abd-el-Fattah & Henderson 1978) we studied the reciprocal group of phenomena which appear when a shock refracts at a fast–slow interface. For this case the gases were conveniently chosen to be air/SF_6 and He/CO_2. By studying the polar diagrams we were able to classify the phenomena into four groups which were also distinguished by different ranges of ξ_i.

In the present paper we return to slow–fast refractions and extend our experiments to values of ξ_i other than $\xi_i = 0{\cdot}5$, with the object of covering all the phenomena which are likely to appear in gases which are nearly perfect. We found it convenient to use a CO_2/CH_4 interface, and after studying the polar diagrams we classified the wave systems into three groups called 'very weak', 'weak' and 'strong'. We selected the following values of ξ_i as representative of each group: $\xi_i = 0{\cdot}78$, $0{\cdot}53$ and $0{\cdot}18$ respectively. In the very weak group we found a free precursor system which apparently has not been previously reported; it appears to be a combination of a weak Mach reflexion† and free precursor shocks. Two other new phenomena were found in the other groups. One was characterized by having two more or less symmetrically placed Mach reflexions in the CO_2. We called it a twin Mach refraction *TMR* to distinguish it from the double Mach refraction *DMR* which was reported in our 1978 paper. In the case of *DMR* the Mach reflexions are in series with each other and appear in the disturbed gas downstream of *i*, whereas in *TMR* they are in parallel and appear in the undisturbed CO_2. The other phenomenon we have called a lambda shock refraction *LSR*. This occurred near glancing incidence as one Mach reflexion became degenerate. We present experimental data on the refractions and their transitions in all the groups and some schlieren photographs of the new phenomena.

2. The very weak group

For this group the experiments were done with an average value of $\xi_i = 0{\cdot}78$ and with ω_0 varying from a comparatively small value near head-on incidence ($\omega_0 \to 0$) to a value near glancing incidence ($\omega_0 \to 90°$). The sequence of events is illustrated in figure 2 and the experimental data in figure 3. The first system is a regular refraction with a reflected expansion wave *e* (*RRE*) and there is a unique solution for it, namely ϵ_1 in figure 2(*a*). This contrasts with our work on the CO_2/He interface for in that case there were two solutions for *RRE* which we labelled ϵ_1 and ϵ_2. We found that it was the weaker solution ϵ_1, i.e. the one with the smaller entropy production $\dot{S}$, which agreed with experiment. In the present case the solution ϵ_1 also agrees well with experiment (figure 3). If ω_0 is now increased then *e* begins to weaken until it eventually becomes a Mach-line degeneracy (figure 2*b*), and at still larger ω_0 it changes continuously into a shock *r* (figure 2*c*), giving the *RRR* system. The polar diagrams show that there are two solutions α_1 and α_2 for *RRR* but it is the α_1 solution which agrees with experiment. This is again the solution with smaller $\dot{S}$. Theory suggests that the transition $RRE \leftrightarrow RRR$ takes place when *i* maps into the intersection point A_1 between the two primary polars; we denote the coincidence by $i \equiv A_1$, and physically it corresponds to the shock impedances of the two gases becoming equal (Henderson 1970). The data support the theoretical prediction of transition.

With further increases in ω_0, a tangency condition forms between the reflected *r* shock polar and the primary *t* polar, so that $\alpha_{1,2}$ form a double root ($\alpha_1 \equiv \alpha_2$, figure 2*d*), and for still larger ω_0 both solutions cease to exist (figure 2*e*). The refraction is now a bound precursor type *BPR*, but we are not sure whether it is $\alpha_1 \equiv \alpha_2$ that defines the transition $RRR \leftrightarrow BPR$ or whether it is a nearby condition where α_1 coincides with a sonic point on either of the *t* or *r* polars. The two conditions are too close together to

† Subsequently we substitute the term 'von Neumann reflexion' *NR* for 'weak Mach reflexion'.

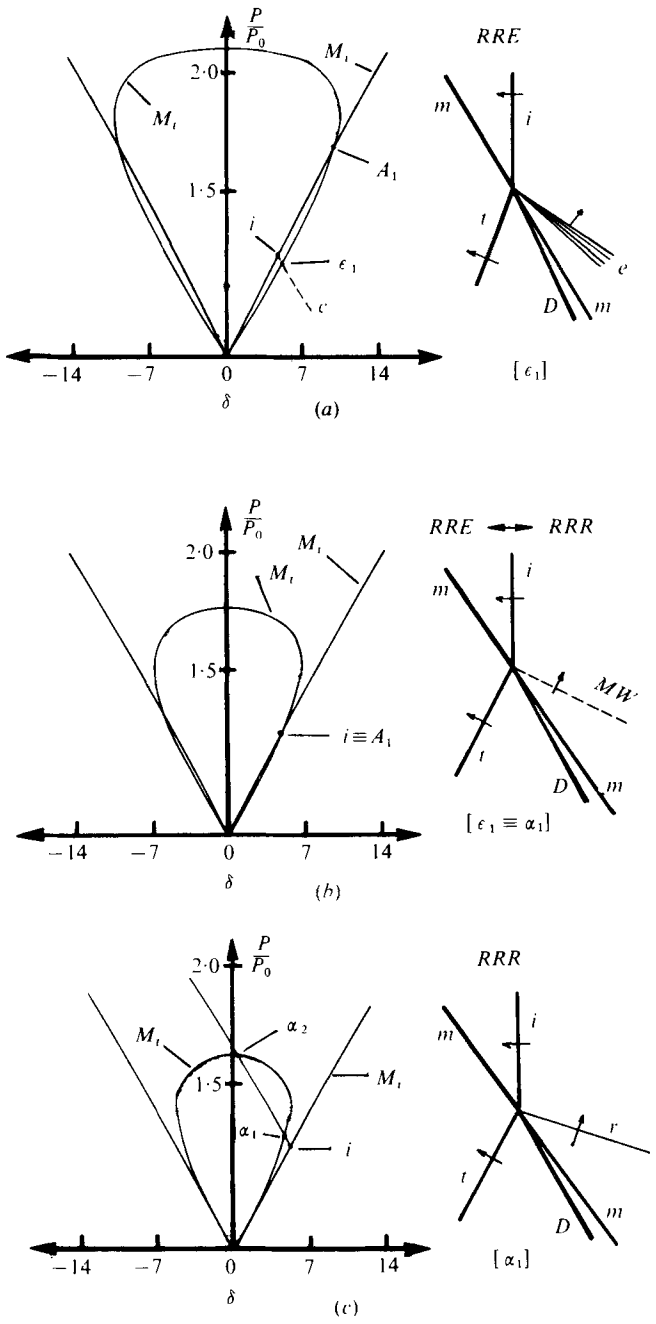

FIGURES 2 (*a–c*). For legend see facing page.

be resolved by our experiments, but transition certainly occurs within this neighbourhood. Our *BPR* data are shown in figure 3 but there is no adequate theory for them yet.

At even larger ω_0, t moves along the interface faster than i does, i.e. t becomes a free precursor. The t shock is itself refracted and transmits a new shock j back into the CO_2 (figure 2*f* and figure 4, plate 1). This system will be thought of as a combination

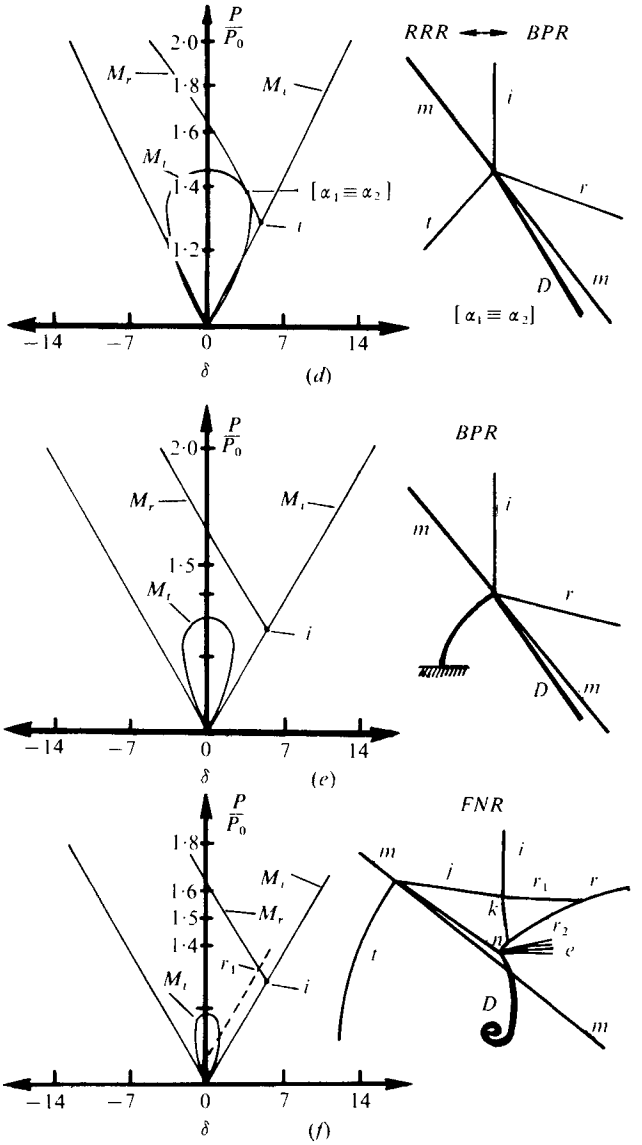

FIGURE 2. Polar diagrams for very weak shock refraction with $\xi_i = 0{\cdot}78$ at a contaminated CO_2/CH_4 gas interface (10 % contamination of the CH_4 by the CO_2). (*a*) Regular refraction solution ϵ_1 with a reflected expansion wave *e* (*RRE*) at $\omega_0 = 31{\cdot}00°$. (*b*) Condition ($\epsilon_1 \equiv \alpha_1$) which determines the transition $RRE \leftrightarrow RRR$ at $\omega_0 = 34{\cdot}37°$. (*c*) Regular refraction solution α_1 with a reflected shock *r* (*RRR*) at $\omega_0 = 36{\cdot}00°$. (*d*) Condition ($\alpha_1 \equiv \alpha_2$) which actually or nearly determines the transition $RRR \leftrightarrow BPR$ at $\omega_0 = 37{\cdot}83°$. (*e*) Irregular refraction of the bound precursor type *BPR*. (*f*) Free precursor von Neumann irregular refraction *FNR*. $M_{i,r,t}$, polar diagrams for the shocks *i*, *r*, *t*; *c*, characteristic map of the expansion *e*; A_1, intersection point of the primary (*i*, *t*) polars; P_0, undisturbed pressure; *P*, disturbed pressure; δ, streamline deflexion angle. For other symbols see caption to figure 1.

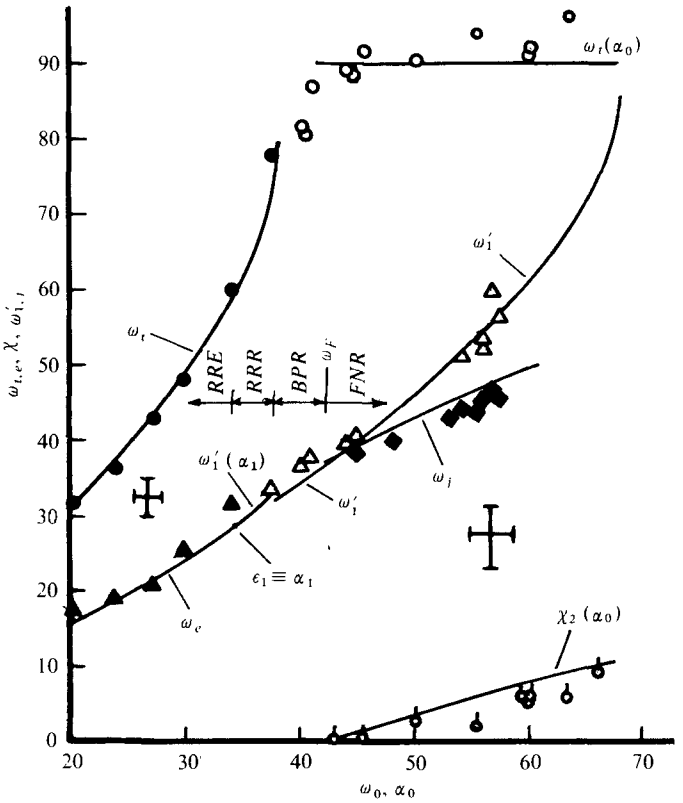

FIGURE 3. Comparison of theoretical and experimental results for the refraction of a very weak $\xi_i = 0{\cdot}78$ plane shock wave at a contaminated CO_2/CH_4 interface. ——, theoretical results; ●, ⊙, experimental data for ω_t for regular and irregular wave systems respectively; ▲, △, experimental data for the wave angles of the leading wave in the reflected expansion e and the reflected shock r, respectively; ◆, wave angle ω_j of the j precursor shock; ○, experimental data for the trajectory path angle χ_2; +, magnitude of the experimental error. For other symbols see captions to figures 1 and 2.

of the t and j precursors and a Mach reflexion. The latter is 'weak' in the strict sense defined by von Neumann (1943) and it is well known that the theory provides no solution in this case (Bleakney & Taub 1949; Guderley 1947, 1962; Sakurai 1964; Henderson & Lozzi 1975). Von Neumann called weak Mach reflexions 'extraordinary Mach reflexions', but it seems appropriate to replace this awkward term with 'von Neumann reflexions', so we shall call the system shown in figure 4, a 'free precursor von Neumann refraction' *FNR*. It has not been previously reported although a closely related free precursor refraction *FPR* was discovered by Jahn (1956) with air/CH_4, by ourselves (1976) with CO_2/He, and also in the present experiments (figure 5, plate 1). The *FPR* system will be discussed in the next section.

Referring to figures 2(*f*) and 4, an expansion e propagates back into the CO_2 from the point where the shock n encounters the interface: it is analogous to a shock reflecting off the edge of a free jet with constant ambient pressure. However the *FNR* is unsteady and the flow downstream of n is subsonic, therefore e can partly overtake n and cause some attenuation. The photograph indicates that further attenuation,

particularly of r, is being caused by the corner signal overtaking it and causing it to curve. In any event the wave angles ω_1' and ω_j of r and j are negligibly different from the local Mach angles μ_1 and μ_j (figure 3). The t shock is very closely a circular arc and therefore is nearly at glancing incidence $\omega_t \approx 90°$ to the interface (figure 3). In our 1976 paper we formulated a piston theory for a wave of this type and applied it to the FPR system. It was based upon the assumption that the piston velocities V_{Pi} and V_{Pt} of the i and t shocks were equal: $V_{Pt} = V_{Pi}$. This made it possible to calculate the radial velocity V_t of t for a given V_i (the velocity of i normal to itself) and then the inverse strength ξ_t of t and the t polar. We can do the same thing for FNR and then calculate the trajectory path angle χ_2 of the confluence of the i and j shocks. The agreement is within the limits of experimental error (figure 3).

The transition $BPR \leftrightarrow FNR$ can be calculated with the help of Snell's law, for since $V_{i,t}$ are the velocities of i and t normal to themselves, and since i and t move along the interface at the same velocity V in BPR,

$$V = V_i/\sin\omega_0 = V_t/\sin\omega_t. \tag{1}$$

But at transition $\omega_t = 90°$, and therefore its critical angle $\omega_0 = \omega_F$ can be found from (1) as

$$\omega_F = \sin^{-1}(V_i/V_t), \tag{2}$$

which gives $\omega_F = 42{\cdot}5°$ in agreement with experiment (figure 3).

All the wave systems in this group were studied for self-similarity by cross-plotting the data in various ways and by examining numerous photographs. We concluded that within the limits of experimental error all the wave systems are closely self-similar.

3. The weak group

The experiments for this group were done with an average value of $\xi_i = 0{\cdot}53$, and with increasing ω_0 we successively obtained the phenomena RRE, RRR and BPR. Qualitatively, they and their transitions are the same as the previous group, so we have omitted them from the sequence shown in figure 6. The range of ω_0 for which RRR exists is now quite small, being only about 1° near $\omega_0 = 37°$. The experimental data are presented in figure 7; the regular refraction theory is in good agreement with these data and so is the transition theory. Beyond the BPR range we obtained a free precursor refraction FPR of the same type as that observed by Jahn (1956, plate 7), by ourselves (1976, plate 2) and here (figure 5). A careful inspection of figures 4 and 5 reveals basic differences between the FNR and FPR systems. In both cases i is modified by the j shock, but in FNR the modified shock k undergoes a von Neumann reflexion as it approaches the gas interface, whereas in FPR it propagates essentially undisturbed to the interface. The property which determines whether a free precursor system is an FNR or an FPR is whether the flow downstream of the modified wave is subsonic or supersonic at the interface. It is subsonic for the former and supersonic for the latter, and we shall define this also to be the difference between the very weak and weak groups. The transition $BPR \leftrightarrow FPR$ is similar to $BPR \leftrightarrow FNR$, and (2) gives $\omega_F = 45{\cdot}9°$ in good agreement with experiment (figure 7).

Here also the j wave was found to be virtually a Mach wave, so that $\omega_j \approx \mu_j$ (figure

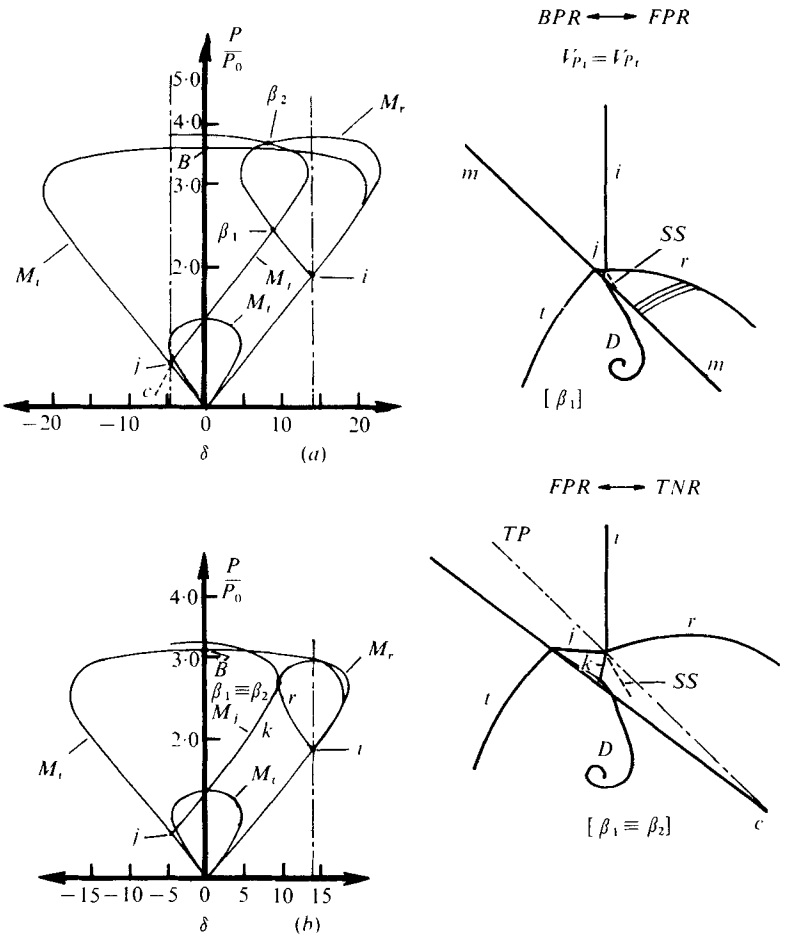

FIGURES 6 (*a*, *b*). For legend see facing page.

7), and for *FPR*, $\omega_t \approx 90°$. The theory for χ_2 agreed with the data within the limits of experimental error, although a small systematic discrepancy was apparent. This may have been due to lack of definition in our photographs, making our measurements subject to a comparatively large error, $\pm 4\frac{1}{2}°$. To our surprise we found that the ω_1' data were significantly stronger than those for a Mach wave, and this caused us to alter our opinion on the nature of the *FPR* system. Referring to figure 2(*f*), we believe that the *FNR* system would be converted into an *FPR* system if the *n* shock were to grow and the *k* shock were to shrink until *n* joined *j* and if the two reflected shocks $r_{1,2}$ were to coalesce into the single *r* shock at the juncture. This would mean of course that *r* would be stronger than a Mach wave, as indeed it is. Unfortunately we were unable to proceed further because the β_1 solution constructed from it (figure 6*a*) was not in good agreement with the data (figure 7). In order to explore the matter further we took a closer look at our assumption that $V_{Pt} = V_{Pi}$, which in effect neglects the piston velocity of the reflected waves. We plotted V_t/V_i against ω_0 for the experimental data (figure 8). Now if it were true that $V_{Pt} = V_{Pi}$ then V_t/V_i would be a constant† which could be calculated; in fact the constant(s) are compared with the data for all

† Note that in general $V_t/V_i \neq 1$ because *i* and *t* propagate in different gases.

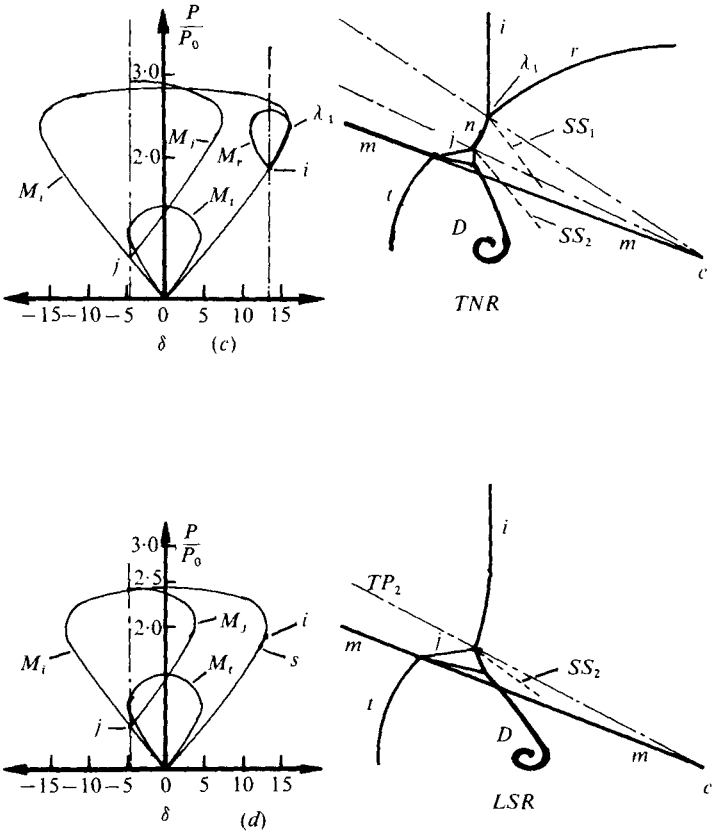

FIGURE 6. Polar diagrams for the weak shock refraction with $\xi_i = 0{\cdot}53$ at a contaminated CO_2/CH_4 gas interface (10 % contamination of the CH_4 by the CO_2). (*a*) The transition $BPR \leftrightarrow FPR$ at $\omega_0 = 45{\cdot}92°$. (*b*) Condition ($\beta_1 \equiv \beta_2$) which actually or nearly determines the transition $FPR \leftrightarrow TNR$ at $\omega_0 = 52{\cdot}70°$. (*c*) Twin von Neumann irregular refraction TNR at $\omega_0 = 56{\cdot}00°$. (*d*) Lambda shock irregular refraction LSR at $\omega_0 = 63{\cdot}00°$. $\beta_{1,2}$, solutions of the four-shock confluence in CO_2 determined by the intersections of the j and r polars. For other symbols see captions to figures 1–3.

three values of ξ_i in figure 8. We see that the assumption $V_{Pt} = V_{Pi}$ is reasonable for $\xi_i = 0{\cdot}78$ for nearly all ω_0, but that for other ξ_i it becomes inadequate as ω_0 becomes larger, in which case the piston velocity of r needs to be considered. So far we have not found a satisfactory way of doing this, and it needs to be born in mind that the problem is complicated at larger ω_0 by the corner signal attenuating r at the wave confluence.

If ω_0 is now subject to further increases we eventually get a third type of free precursor system which we also believe not to have been reported before (figure 6*c*); a photograph of this is shown in figure 9 (plate 2). It features a pair of von Neumann reflexions in the CO_2 and we name it a 'twin von Neumann refraction' TNR. Figure 7 shows that here r remains virtually a Mach wave, and the solution λ_1 obtained from the piston theory for ω_1 is even more unsatisfactory than for FPR, but the discrepancy for χ_2 is small. There is now an extra trajectory path angle χ_1 for the upper reflexion. A very simple theory for χ_1 can be constructed by noting the experimental fact that

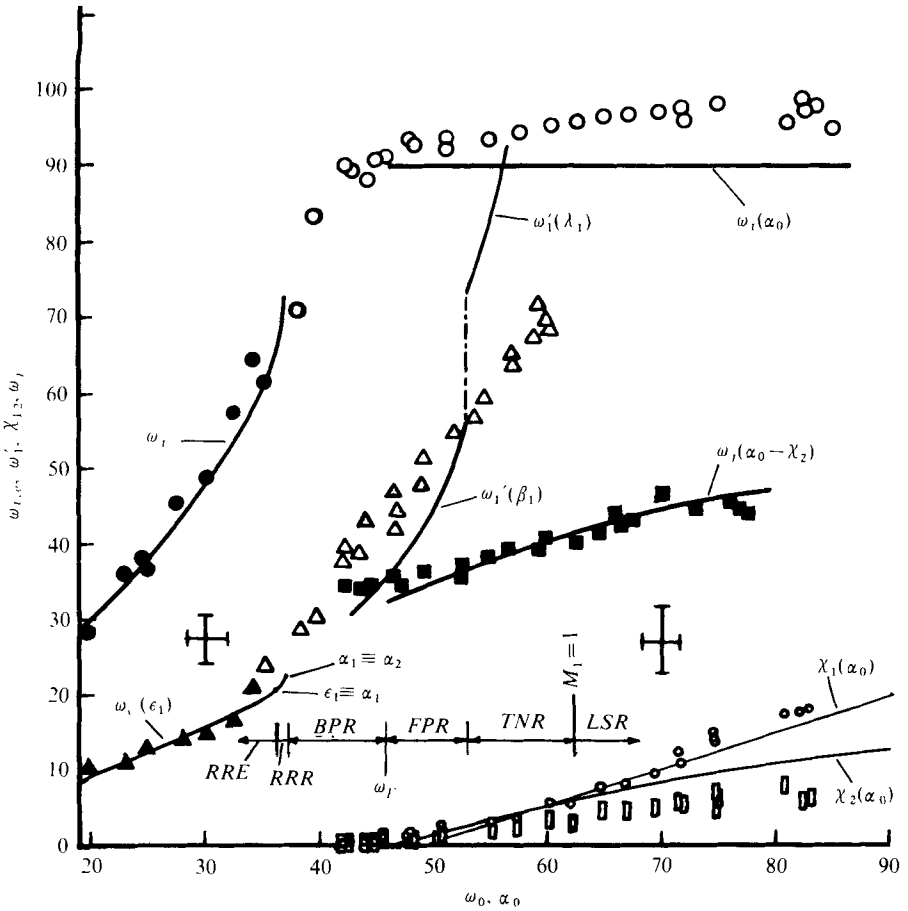

FIGURE 7. Comparison of theoretical and experimental results for the refraction of a weak $\xi_i = 0{\cdot}53$ plane shock wave at a contaminated CO_2/CH_4 interface. ■, experimental data for the wave angle ω_j of the j precursor; ⊙, ⊡, experimental data for the trajectory path angles $\chi_{1,2}$ respectively. For other symbols see captions to figures 1–3 and 6.

once the corner signal has everywhere overtaken r the trajectory of the i, r, n confluence becomes independent of the *set* angle of incidence α_0. Kawamura & Saito (1956) noticed the same effect during their experiments with shock wave diffraction. If $\omega_0 = \omega_c$ is the critical angle at which the corner signal first reaches the confluence point then from the geometry of the system we have

$$\chi_1 = \omega_0 - \omega_c. \tag{3}$$

This formula gives good results as shown in figure 7.

Referring again to figure 7, it will be seen that the piston theory is accurate enough to predict the transition $FPR \leftrightarrow TNR$. It will be noted that β_1 becomes unreal at or near this condition, which suggests that the condition is determined by the double root (tangency) $\beta_1 \equiv \beta_2$ or by a near coincidence of β_1 with a sonic point. Although the alternatives are again too close together to be resolved in our experiments, nonetheless transition does take place close to the theoretical value $\omega_0 = 52{\cdot}7°$ (figure 7). It is

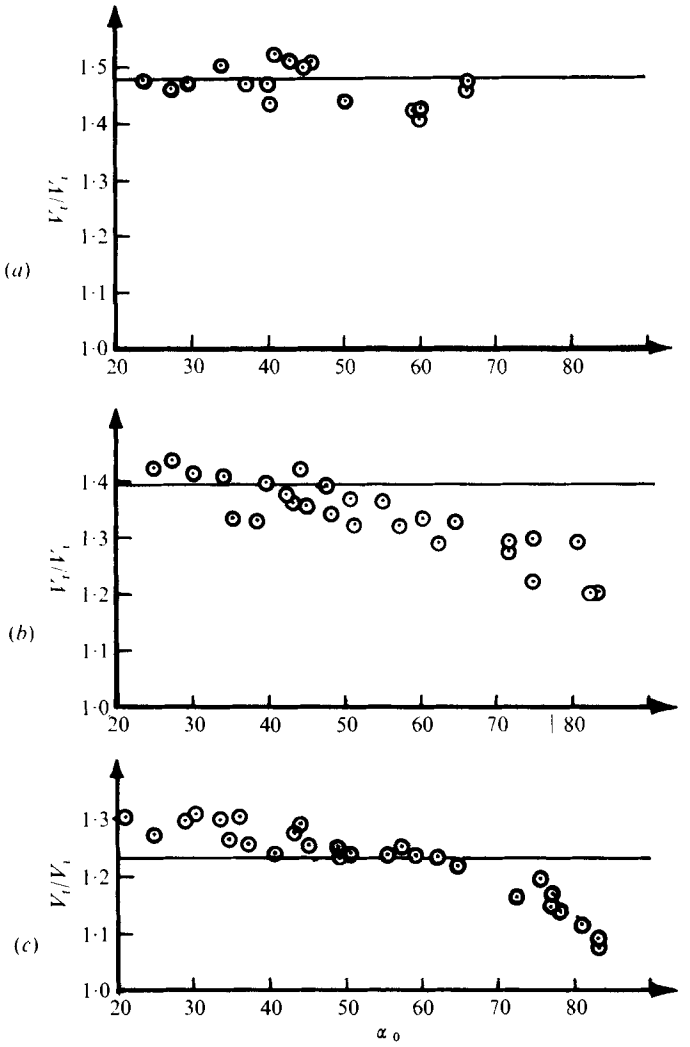

FIGURE 8. Comparison of the theoretical and experimental results for the velocity ratio V_t/V_i of the incident and transmitted shocks against the set angle of incidence α_0. (*a*) $\xi_i = 0{\cdot}78$. (*b*) $\xi_i = 0{\cdot}53$. (*c*) $\xi_i = 0{\cdot}18$. ——, theory based upon the assumption $V_{pt} = V_{pi}$; ⊙, experimental data.

important to note from figure 6 that transition occurs *inside* the main CO_2 polar, which means physically that the pressure downstream of r and k at transition will be less than that behind a normal shock B in the CO_2. We denote this fact by ord $(\beta_1 \equiv \beta_2)$ < ord B, where 'ord' stands for 'ordinate of'. This topological property is actually the definition of a weak incident shock and therefore it is an essential property of the two weak groups. As explained in our 1978 paper, it is a generalization of the von Neumann (1943) classification. By contrast, the strong group has

$$\text{ord}\,(\beta_1 \equiv \beta_2) > \text{ord}\,B,$$

and the boundary between the weak and the strong group is evidently

$$\text{ord}\,(\beta_1 \equiv \beta_2) = \text{ord}\,B.$$

The practical importance of this distinction is that the von Neumann theory agrees well with the experimental data on the Mach reflexions in the strong group, but it fails for the von Neumann reflexions in the weak groups. In the latter case we have made what use we can of the piston theory.

At still larger ω_0 the free-stream Mach number M_1 downstream of i begins to approach unity, and at $\omega_0 = 62{\cdot}46°$ theoretically $M_1 = 1$. This means that r degenerates to a Mach wave, and if ω_0 becomes any larger then there is at most only unsteady sonic disturbances. A photograph of a refraction of this type is shown in figure 10 (plate 2), and because of its shape we shall call it a lambda shock refraction *LSR* (figure 6*d*). As far as we know it has not been reported before. Evidently the transition $TNR \leftrightarrow LSR$ occurs at $M_1 = 1$.

The wave systems in this group were also studied for self-similarity by cross-plotting the data in various ways. We concluded that all except the *LSR* were self-similar. Signs of loss of self-similarity began to appear when $\omega_0 > 72°$ and it was manifested by V_t becoming smaller as ω_0 increased, so that t moved ahead of i at a slower rate as glancing incidence was approached.

4. The strong group

The experiments for this group were done with ξ_i held constant at $\xi_i = 0{\cdot}18$. Part of the sequence is shown in figure 11 and the data are shown in figure 12. Here also the theory is in good agreement with the regular refraction data. In this case it was possible to measure the deflexion angle δ_t of the gas interface with reasonable accuracy, and the theory is in good agreement. This gives confidence that the theory is predicting the strength of the reflected expansion e correctly. The leading and final waves of e are not well defined in the photographs and cannot be measured with precision. There is no *RRR* system in the series so we have the transition $RRE \leftrightarrow BPR$. The polar maps show that for the part of the range beginning at $i \equiv A_1$ there are two solutions ϵ_1 and ϵ_2 for *RRE*, but as with our 1976 experiments we found that it was the smaller S solution ϵ_1 which agreed with the data. With increasing ω_0 the double solution $\epsilon_1 \equiv \epsilon_2$ is obtained in which the characteristic c which is the map of e forms a tangency point with the primary CH_4 polar, and it is this condition which determines $RRE \leftrightarrow BPR$.

For values of ω_0 beyond the *BPR* range we obtained a refraction system similar to the *TNR* system except that now there are twin Mach reflexions instead of twin von Neumann reflexions. The new system will be called a *TMR*. The von Neumann three-shock theory is applicable to *TMR* because i is now a strong shock. In fact the solution of the upper wave confluence is given by the point λ_1 in figure 9(*b*) and determines both ω_1' and the local wave angle ω_{ni} of the Mach stem n at the confluence. The agreement is good (figure 12). Interestingly, the calculations for ω_1' can now be extended back into the *BPR* range. The angle is harder to measure for *BPR* so the data are more scattered, but the agreement is good except near the transition $RRE \leftrightarrow BPR$, where according to the theory the *RRE* and *BPR* solutions are not continuations of each other. Incidentally this is the first time that we have been able to calculate a wave angle in *BPR* with any degree of success. The χ_2 theory remains good, but the χ_1 theory (3) is unsatisfactory. The transition $BPR \leftrightarrow TMR$ at $\omega_0 = \omega_F$ is given by (2) as $\alpha_F = 56{\cdot}6°$, which agrees well with the data (figure 12). For still larger ω_0 when $M_1 < 1$ we obtained the *LSR* system as with the weak group.

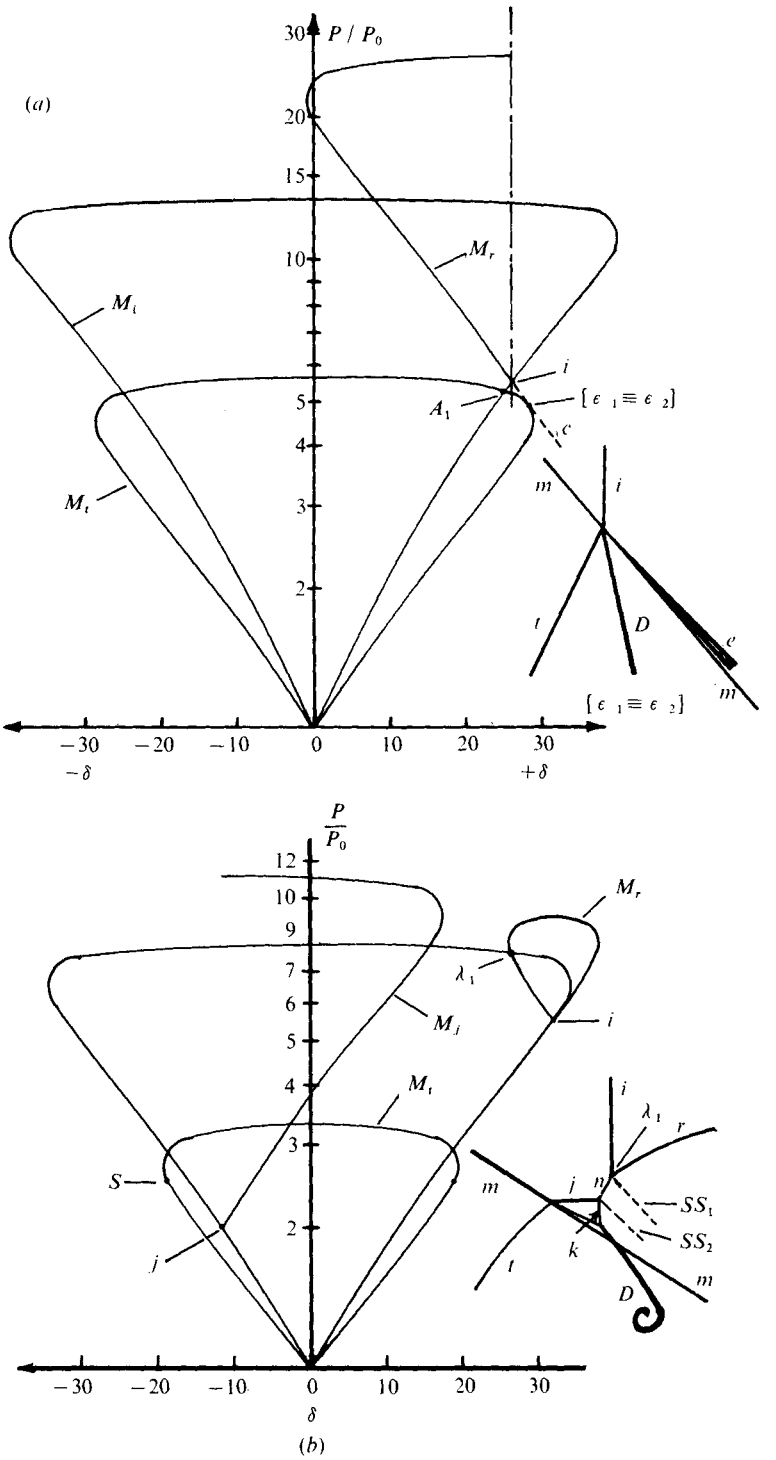

FIGURE 11. Polar diagrams for the strong shock refraction with $\xi_i = 0{\cdot}18$ at a contaminated CO_2/CH_4 gas interface (10 % contamination of the CH_4 by the CO_2). (*a*) The transition $RRE \leftrightarrow BPR$ at $\omega_0 = 40{\cdot}30°$, defined by $\epsilon_1 = \epsilon_2$. (*b*) Twin Mach reflexion irregular refraction TMR at $\omega_0 = 56{\cdot}50°$. For other symbols see captions to figures 1–3, 6 and 7.

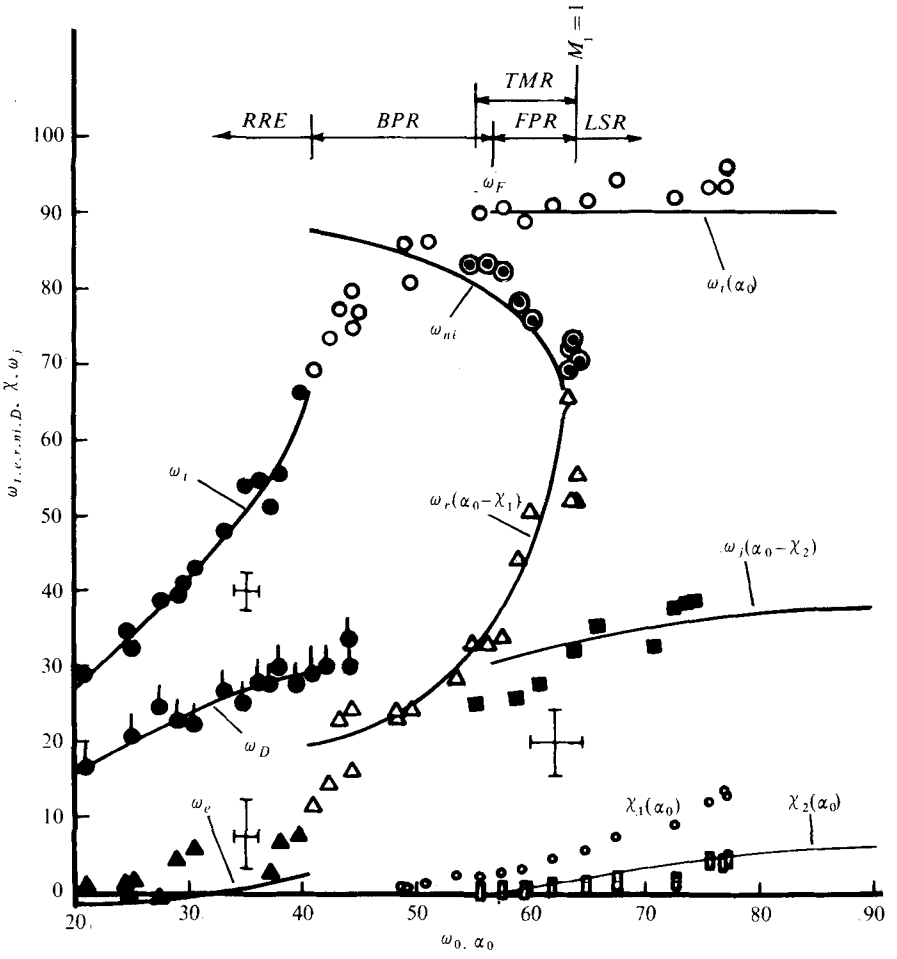

FIGURE 12. Comparison of theoretical and experimental results for the refraction of a strong $\xi_i = 0{\cdot}18$ plane shock wave at a contaminated CO_2/CH_4 interface. For symbols see captions to figures 1–3, 6 and 7.

The definition of the schlieren photographs was a little better in these experiments than in our earlier ones and we could see something of the *BPR* structure. It seems to have the same form as *TMR*, although of course *t* is a bound precursor and not a free one. We also studied the interferometer photographs in Jahn's paper and particularly his plates 5, 6 and 12, which all appear to be bound precursor systems. Although the definition of the interferometer photographs does not equal that of the schlieren photographs, we suggest that the *BPR* system in his plate 5 is structurally the same as ours. At larger ω_0 Jahn obtained a second *BPR* system distinguished by a single Mach reflexion (plates 6 and 12 of his paper). Thus for an air/CH_4 interface with $\xi_i = 0{\cdot}3$ he found two types of *BPR*, whereas we found only one with $\xi_i = 0{\cdot}18$ at a CO_2/CH_4 interface. We obtained the *TMR* and *LSR* systems at larger ω_0 whereas he obtained the single Mach reflexion *BPR*. Presumably our results would change into those of Jahn if we were to dilute the CO_2 in our experiments continuously with air

until the air had entirely replaced the CO_2, and at the same time continuously changed ξ_i from 0·18 to 0·3.

There was a partial loss of self-similarity for all the wave systems in this group owing to the reflected waves becoming stationary at or near the corner. However all the systems except *LSR* appeared to be self-similar away from the corner. For $\omega_0 > 70°$ there was a noticeable loss of self-similarity for the *LSR* system, the *t* shock slowing down relative to *i* with increasing ω_0.

5. Concluding remarks

5.1. *Slow–fast refraction*

It was concluded that the refraction phenomena at a slow–fast interface could be conveniently classified into three groups, assuming that the gases were nearly perfect. In the first of them, the very weak group, there are two regular refractions, one with a reflected *RRE* and the other with a reflected shock *RRR*. There is also a bound precursor refraction *BPR* and a free precursor refraction *FNR* which can be regarded as a combination of a von Neumann *reflexion* and free precursor *t* and *j* waves. In the second group, the weak group, there are also *RRE*, *RRR* and *BPR*, but there are three free precursor systems *FPR*, *TNR* and *LSR*. The *FPR* differs from the *FNR* in that the flow downstream of the *k* shock is supersonic in the former and subsonic in the latter, and this distinguishes the two weak groups. For larger incidence angles ω_0, the *FPR* changes into the twin von Neumann refraction *TNR* and at still larger ω_0 one of the reflexions becomes degenerate, the free-stream Mach number downstream of the incident shock *i* becoming subsonic. We then obtained the lambda shock refraction *LSR*. In the third group, the strong group, there are again *RRE*, *BPR* but no *RRR* or *FPR*. There are two *BPR* systems at an air/CH_4 interface according to Jahn, but only one at a CO_2/CH_4 interface according to us. The first free precursor system now has twin Mach reflexions *TMR* instead of von Neumann reflexions. Subsequently, with increasing ω_0, the *TMR* system degenerates into the *LSR* system. Finally some critical curves which define the transition conditions for many of the phenomena at a CO_2/CH_4 interface are shown in figure 13.

5.2. *Fast–slow refraction*

In our 1978 paper we found that the same classification method led to two classes which we called weak and strong and that both of these could be further divided into two subclasses, resulting in four groups of phenomena in all. They were referred to as the very weak, the weak, the strong and the stronger groups. We obtained data and photographed the phenomena in every group. In the very weak group we found some conflict with Jahn's experiments. He obtained an interferometer photograph of an irregular system which was characterized by a dispersed (non-centred) reflected expansion. We found that this system could be suppressed by reducing membrane leakage and improving our downstream boundary conditions. In its place we found a new irregular system with a centred (and curved) reflected expansion *CER*. By contrast our photographs were taken with a schlieren system. In the weak group the irregular refraction was a Mach-reflexion type *MRR* but with no sign of a vortex sheet. This property had been foreshadowed by von Neumann, who seemingly implied that it was a new type of Mach reflexion. For the strong group we again obtained *MRR* as an

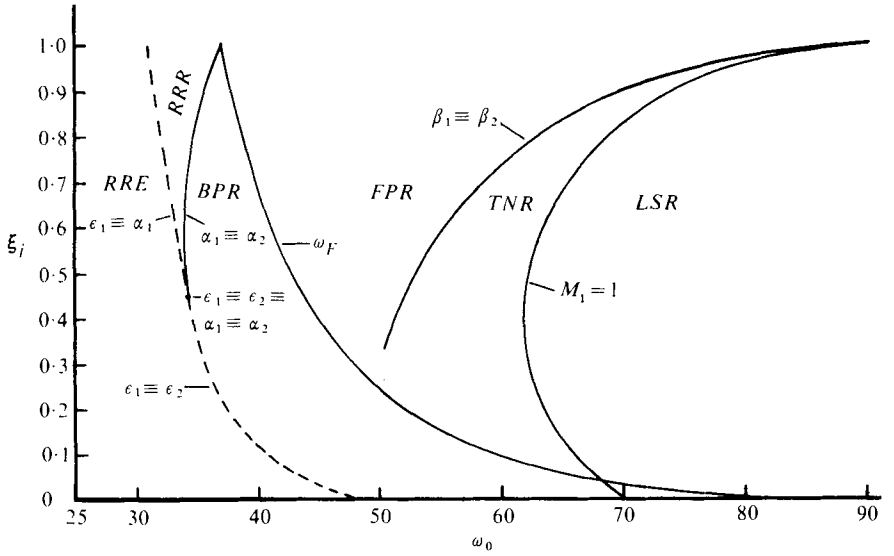

FIGURE 13. Topological map of the conditions which determine each phenomenon which occurs during the refraction of a plane shock wave at an uncontaminated CO_2/CH_4 interface. For symbols see captions to figures 1–3, 6 and 7.

irregular refraction but with the difference that the vortex sheet was now visible. Near glancing incidence the Mach number of the flow downstream of the reflected shock becomes smaller than one ($M_1 < 1$) so the *MRR* system cannot then exist. For an air/SF_6 interface this happens for $\omega_0 > 61{\cdot}76°$, and for this condition we found another new system *CFR* in which the incident shock was curved concave forwards and emitted a continuous band of reflected compression waves behind it. The photograph of it, which we published in figure 11 of that paper, shows not only the wavelets but also a band of vortex sheets propagating from the shock. For the stronger shock group we found that the Mach number of the flow *downstream* of the reflected shock was supersonic ($M_2 > 1$) for a small range of ω_0, and for this condition the refraction contained a double Mach reflexion *DMR*. The analogous system has often been observed during the reflexion and diffraction of shocks over wedges (Gvosdeava *et al.* 1970; Law & Glass 1971; Henderson & Lozzi 1975), but this was the first time it had been observed in refraction.

The theoretical and experimental work presented here and in the papers cited in the references should be sufficient to give a substantially complete picture of all the phenomena involved, at least when the gases are approximately perfect. Of course we cannot be absolutely sure of this and indeed new dimensions would be added by consideration of magneto-gasdynamic effects (Bestman 1977), or chemical reactions leading to detonation waves (Shchelkin & Troshin 1964; Macpherson 1969), or shear waves, or gravitational waves along the gas interface and so on.

This work is supported by the Australian Research Grants Committee.

REFERENCES

ABD-EL-FATTAH, A. M. & HENDERSON, L. F. 1978 *J. Fluid Mech.* **86**, 15.

ABD-EL-FATTAH, A. M., HENDERSON, L. F. & LOZZI, A. 1976 *J. Fluid Mech.* **76**, 157.

BESTMAN, A. R. 1977 *J. Plasma Phys.* **18**, 189.

BLEAKNEY, W. & TAUB, A. H. 1949 *Rev. Mod. Phys.* **21**, 584.

GUDERLEY, K. G. 1947 Considerations of the structure of mixed subsonic–supersonic flow patterns. *Headquarters Air Materiel Command, Wright Field, Dayton, Ohio, Tech. Rep* F-TR-2168-ND.

GUDERLEY, K. G. 1962 *The Theory of Transonic Flow.* Pergamon.

GVOSDEAVA, L. G., BAZHENOVA, T. V., PREDVODITELEVA, O. H. & FOKEEV, V. P. 1970 *Astron. Acta* **15**, 503.

HENDERSON, L. F. 1967 *J. Fluid Mech.* **26**, 607.

HENDERSON, L. F. 1970 *J. Fluid Mech.* **40**, 719.

HENDERSON, L. F. & LOZZI, A. 1975 *J. Fluid Mech.* **68**, 139.

JAHN, R. G. 1956 *J. Fluid Mech.* **1**, 457.

KAWAMURA, R. & SAITO, H. 1956 *J. Phys. Soc. Japan* **11**, 574.

LAW, C. K. & GLASS, I. I. 1971 *C.A.S.I. Trans.* **4**, 2.

MACPHERSON, A. K. 1969 *Astron. Acta* **14**, 549.

NEUMANN, J. VON 1943 Oblique reflexion of shock waves. *Collected Works*, vol. 6, p. 238. Pergamon.

POLACHEK, H. & SEEGER, R. J. 1951 *Phys. Rev.* **84**, 922.

SAKURAI, A. 1964 *J. Phys. Soc. Japan* **19**, 1440.

SHCHELKIN, K. I. & TROSHIN, YA. K. 1964 Gasdynamics of combustion. *N.A.S.A. Tech. Trans.* no. 231.

TAUB, A. H. 1947 *Phys. Rev.* **72**, 51.

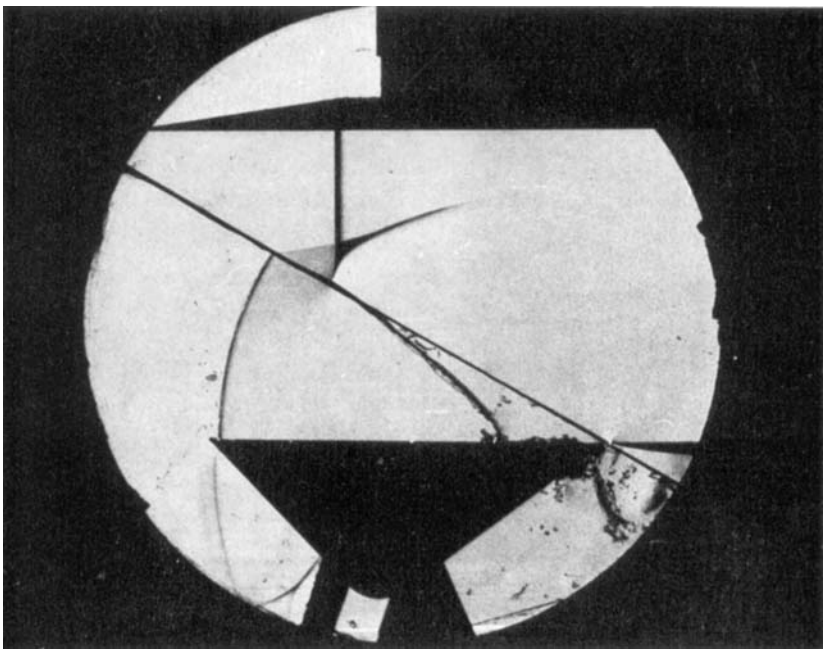

FIGURE 4. Free precursor von Neumann irregular refraction FNR at a CO_2/CH_4 interface with $\xi_i = 0{\cdot}78$.

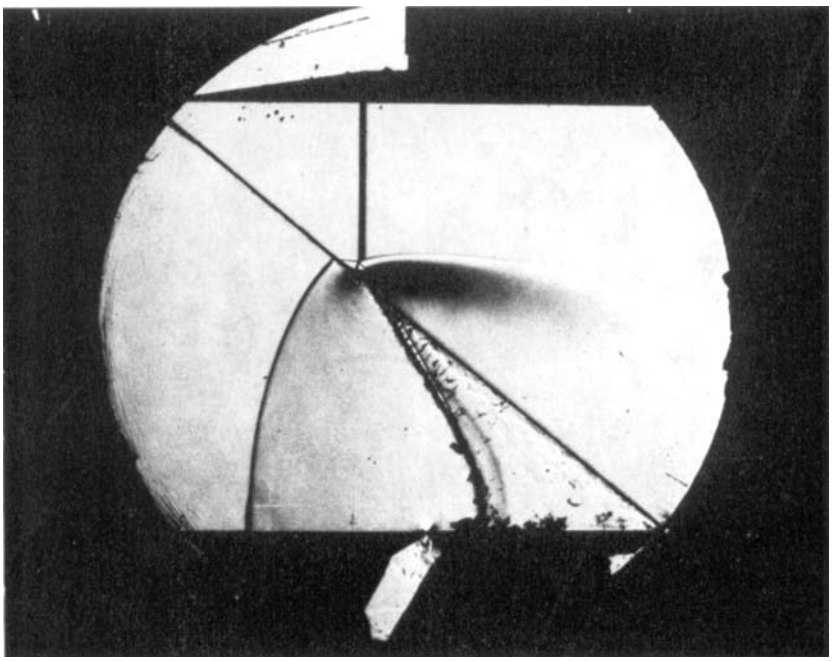

FIGURE 5. Free precursor irregular refraction FPR at a CO_2/CH_4 interface with $\xi_i = 0{\cdot}53$.

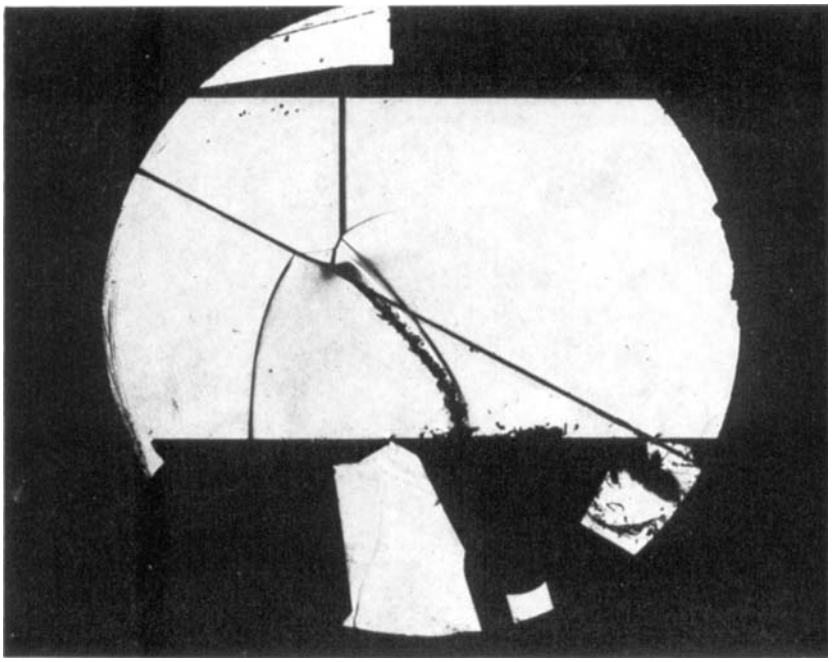

FIGURE 9. Twin von Neumann irregular refraction TNR at a CO_2/CH_4 interface with $\xi_i = 0{\cdot}53$.

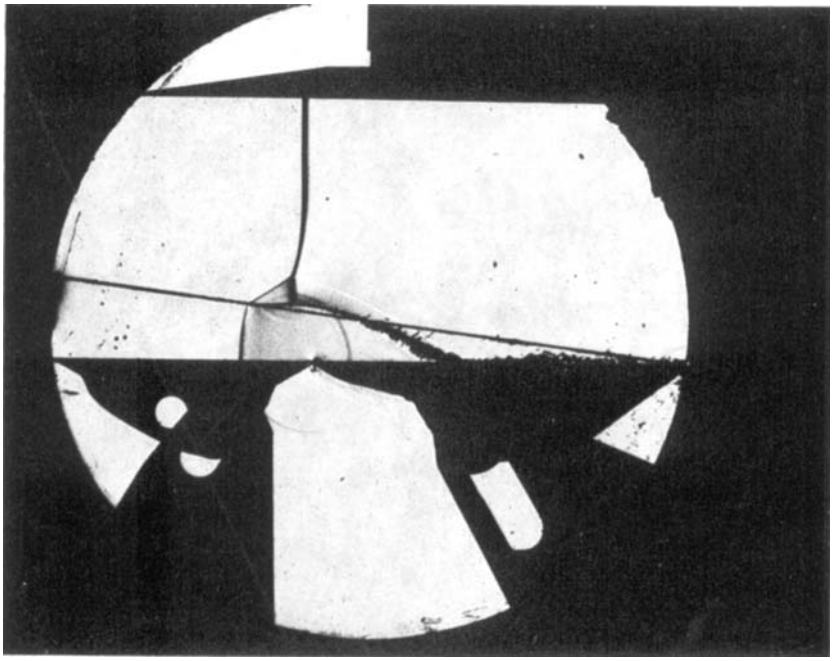

FIGURE 10. Lambda shock irregular refraction LSR at a CO_2/CH_4 interface with $\xi_i = 0{\cdot}53$.